Chapter 4

Preliminary Photophysical Measurements for Fluorescent Molecular Sensors

4. Preliminary photophysical measurements for fluorescent molecular sensors

4.1. Background

The ^{1}H NMR titration experiments for the investigation of host-guest interactions described in the previous chapter showed that the Cd(II) complexes of the fluorescent ligands (**146**, **170**-**172**), do act as capable receptors for a variety of guests in DMSO-d_6. With the ability for guest inclusion confirmed, the ligands (**146**, **170**-**172**), and the receptors **4**–**7** were investigated to examine their potential as molecular sensors. A molecular sensor is a molecular device that is able to detect a specific event, such as guest inclusion, and inform an observer of the occurrence of this event in real time, in this case by a change in fluorescence.

Prior to undertaking a study of the fluorescence perturbation induced in the receptor complex by the incoming guest the fluorescence properties of first the receptor ligand and then the receptor complex needed to be understood.

4.2. Effect of pH on the photophysical properties of the receptor ligands

To observe the influence of pH on the absorption and fluorescence properties of the ligands (**146**, **170**-**172**), a series of titration experiments was conducted. The precursor ligand antac-12 was included in this work for reference purposes. The detailed experimental procedure is outlined in **Chapter 6**. Generally speaking it involved the addition of aliquots of a solution tetraethylammonium hydroxide, (NEt_4OH), to a dilute solution (10^{-6} mol dm^{-3} for fluorescence and 10^{-4} mol dm^{-3} for absorption studies) of each of the protonated (by treatment with perchloric acid)

ligands in 20% aqueous 1,4-dioxane, at a constant ionic strength of I = 0.1 mol dm^{-3} (NEt_4ClO_4), and the measurement of the absorption spectra (over the range 300-500 nm) or the fluorescence emission spectra (over the range 370-550 nm) upon each addition of base. 1,4-Dioxane is a polar, water miscible organic solvent in which the ligands (and their complexes) are soluble at the concentrations required for photophysical studies (from 10^{-6} mol dm^{-3} to 10^{-4} mol dm^{-3}), and which has a good UV transparency (at >220 nm for 1 cm path length).[259]

For fluorescence studies there are two options for determining the wavelength of excitation. In cases where only a single species is under investigation the wavelength of maximum absorbance is usually chosen, to maximise the energy input. In other cases where two fluorescent species are in equilibrium it is usual to choose an isosbestic wavelength, which is a wavelength at which the energy input to both fluorescing species is the same. Because of the expected pH dependent speciation of the fluorescent ligands under investigation here, as partly shown in **Figure 4.1**, it was first of all necessary to record the absorption spectrum at each of various pH values to determine if such an isosbestic point exists. This will be addressed in the next section.

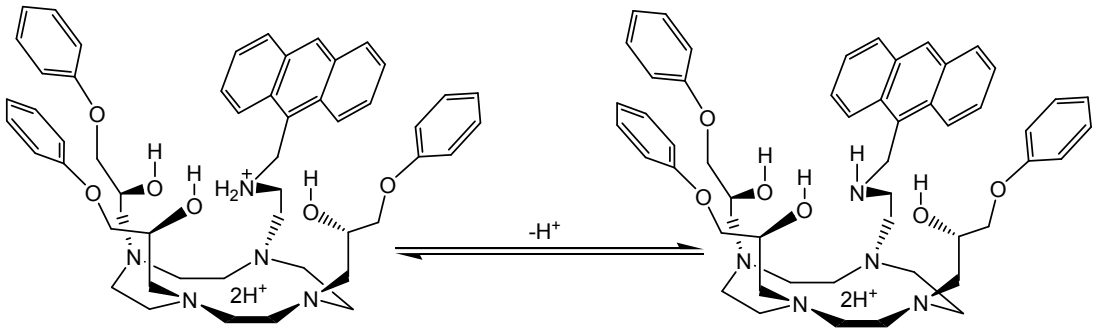

Figure 4.1. The deprotonation of the anthrylamine occurs around pH 7. Other levels of protonation within the cyclen residue are also possible.

4.2.1. Effect of pH on the absorption spectrum of receptor ligands.

The absorption spectra of ligand **146** was recorded as a function of pH, as shown in **Figure 4.2**. The pH values recorded between 2 and 12 were those indicated by a pH meter employing a combination glass electrode calibrated against aqueous buffers. For pH values above 12, indicator paper was used. At constant pH no variations of wavelength over time were observed, allowing any wavelength shifts to be attributed to the pH changes investigated.

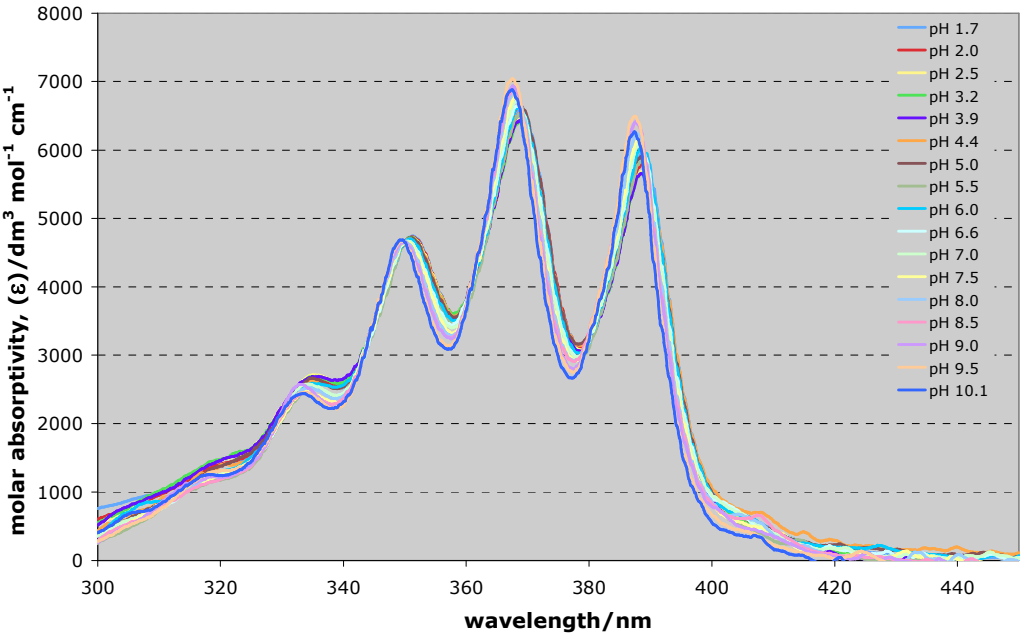

Figure 4.2. The UV-visible absorption spectra for the titration of protonated **146** [1 x 10^{-4} mol dm^{-3}] with NEt_4OH in 20% aqueous 1,4-dioxane (I = 0.1 mol dm^{-3}, NEt_4ClO_4) at 298 K.

As the pH increased the molar absorptivity of the ligand increased at the band maxima, and the wavelengths of the absorption bands were shifted. At an apparent pH of *ca* 1.7 the absorption bands were observed at 387.3, 367.0, 349.2 and 332.4 nm. When these are compared with the absorption bands at pH 10, which are 386.9 366.6, 348.8 and 332.8, it can be seen that treatment with base causes a minor hypsochromic shift (λ→blue) of *ca* 0.4 nm for the more intense bands, at *ca* 387, 367

and 349 nm, and a slight bathochromic shift (λ→red) for the band at *ca* 333 nm, as well as an increase in extinction coefficient (ε) for all bands (a hyperchromic shift). The hyperchromic shift is consistent with an increase in electron delocalisation,[260] as would be expected upon deprotonation of the protonated anthrylamine. These shifts in absorption spectra revealed an isosbestic point at 350 nm, which would be used as the excitation wavelength in future fluorescence work, eliminating any concern over the precise nature or complexity of the speciation of the ligand under the prevailing conditions. The absorption spectra for ligands (**170-173**) were similar, and also showed isosbestic points at 350 nm.

4.2.2. Effect of pH on fluorescence spectra of receptor ligands.

In a similar way to the study of absorbance, the fluorescence spectra of ligand **146** was recorded as a function of pH using the excitation wavelength of 350 nm. At pH 14 the fluorescence emission spectrum appeared as shown in **Figure 4.3**.

Somewhat surprisingly the quantum yield (Φ = 0.069) was considerably higher than for **antac-12**, **131**, recorded under identical conditions, (Φ = 0.028, this work) or that of Kimura and co-workers, who measured a value of Φ = 0.02 in water[151]. This was rationalised in terms of the anthryl N atom acting as a hydrogen bond acceptor for a neighbouring pendant O-H group as shown in **Figure 4.4.** This would tend to direct the nitrogen lone pair electrons towards the donated H atom and disrupt the PeT quenching, thereby enhancing the fluorescence compared to **131**.

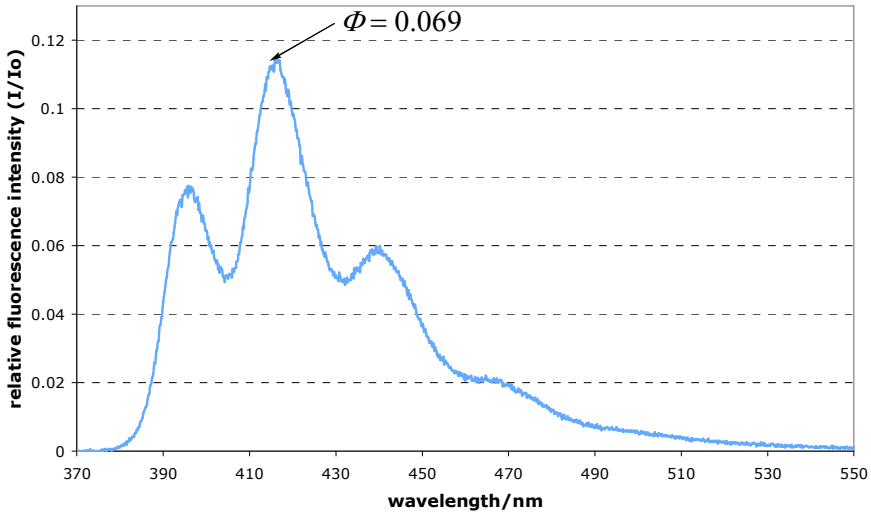

Figure 4.3. The fluorescence emission spectrum of **146** [1 x 10^{-6} mol dm^{-3}], pH 14 in 20% aqueous 1,4-dioxane (I = 0.1 mol dm^{-3}, NEt_4ClO_4) at 298 K when excited at 350 nm. I_o has been referenced as the fluorescence intensity of **4** at pH 7, and has been set to 1.

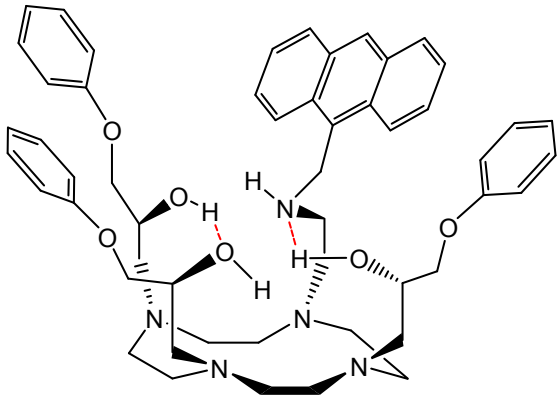

Figure 4.4. Hydrogen bonding within receptor ligand **146**, which would explain its high fluorescence compared to **131**. More elaborate H-bonding schemes are possible.

Acidification of **146** produced an enhancement of the fluorescence as shown in **Figure 4.5(a)** and from this it was evident, as expected, that protonation is capable of blocking the PeT effect much more effectively than hydrogen bond acceptance. The plot of fluorescence emission at λ_{max} versus pH showed a sigmoidal shape (**Figure 4.5(b)**) suggestive of a pH dependent equilibrium between strongly fluorescent species at low pH and more weakly fluorescent species at high pH. A pK_a value of 8.4 ± 0.4 relating these two species, or groups of species, was evident. This pK_a most likely relates to the equilibrium shown in **Figure 4.1** where the anthrylamine, most closely involved with PeT fluorescence quenching, undergoes

protonation or deprotonation. Kimura, in his work with **131**, recorded a pK_a value for this process in water of 7.2 ± 0.2.[151] The difference in these values is attributed to the present value being recorded in the 20% aqueous 1,4-dioxane, where dissociation is weaker. Over the entire pH range investigated there is a small hypsochromatic shift of *ca* 2.1 nm for each of the four emission peaks as the pH is raised. The quantum yield maximises with a value of $\Phi = 0.590$ at pH 3.0, for **131** the maximum was $\Phi = 0.570$ at pH = 3.0.

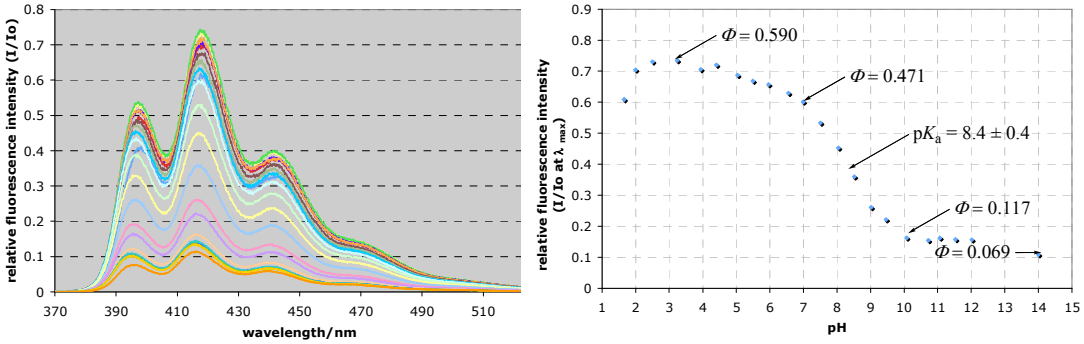

Figure 4.5. (**a**) Fluorescence emission spectra during the titration of protonated **146** [1 x 10^{-6} mol dm^{-3}] with NEt_4OH in 20% aqueous 1,4-dioxane (I = 0.1 mol dm^{-3}, NEt_4ClO_4) at 298 K when excited at 350 nm. Emission maxima are at 398.1, 418.8 and 442.6 nm at pH 3 and 396, 416.7 and 441.2 nm at pH 10. Maximum fluorescence emission intensity decreases from pH 3.0 (green curve) to pH 14.0 (orange curve); (**b**) Fluorescence intensity of **146** at λ_{max} plotted against pH, values derived from **Figure 4.5(a)**. I_o has been referenced as the fluorescence intensity of **4** at pH 7, and has been set to 1.

Quenching was observed for **146**, under strongly acidic conditions (pH < 3), with the diminution much larger than was observed for **131** under the same conditions. This behaviour has been attributed by Czarnik to protonation of an aromatic ring of anthracene.[171]

The fluorescence emission spectrum shown in **Figure 4.6** for neutral **170** (pH 14) indicates a quantum yield (Φ = 0.047), again considerably higher than for **131**, due to the anthrylamine group possibly acting as a hydrogen bond acceptor for a neighbouring pendant O-H group.

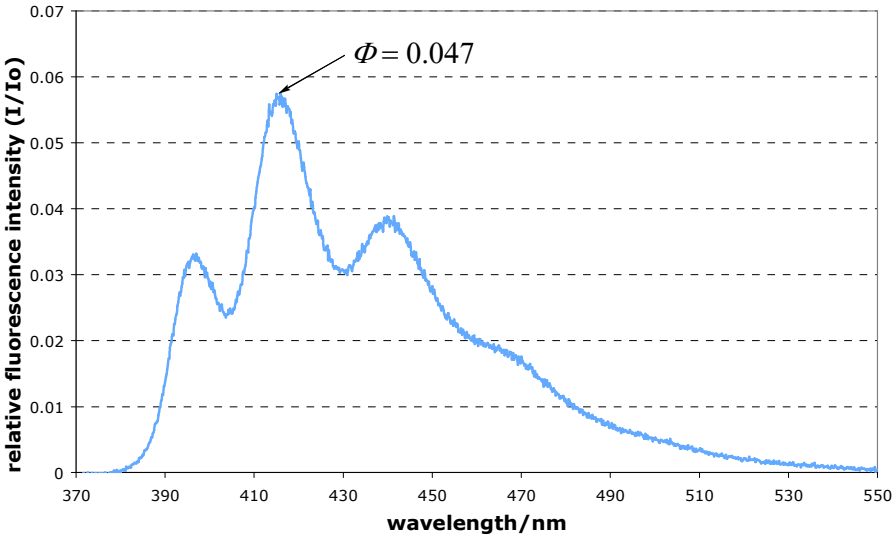

Figure 4.6. The fluorescence emission spectrum of **170** [1 x 10^{-6} mol dm^{-3}] at pH 14 in 20% aqueous 1,4-dioxane (I = 0.1 mol dm^{-3}, NEt_4ClO_4) at 298 K when excited at 350 nm. I_o has been referenced as the fluorescence intensity of **4** at pH 7, and has been set to 1.

As with **146** acidification of **170** produced an enhancement of the fluorescence as shown in **Figure 4.7(a)**. The plot of fluorescence emission intensity at λ_{max} versus pH revealed a pK_a of 8.0 ± 0.3, again most likely associated with protonation/deprotonation of the anthrylamine group and consistent with the value seen in **146**. As with **131** and **146**, quenching was observed under strongly acidic conditions.

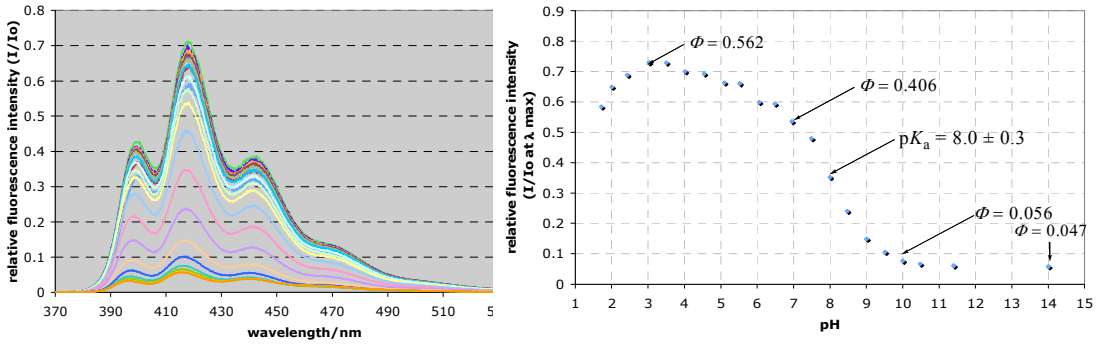

(a) **(b)**

Figure 4.7. **(a)** Fluorescence emission spectra during the titration of protonated **170** [1 x 10^{-6} mol dm^{-3}] with NEt_4OH in 20% aqueous 1,4-dioxane (I = 0.1 mol dm^{-3}, NEt_4ClO_4) at 298 K when excited at 350 nm. λ_{max} values at 400.1, 419.2 and 443.0 nm at pH 3 and at 398.3, 417.1 and 442.0 nm at pH 10. Maximum fluorescence emission intensity decreases from pH 3.0 (green curve) to pH 14.0 (orange curve); **(b)** Fluorescence intensity of **170** at λ_{max} plotted against pH, values derived from **Figure 4.7(a)**. I_o has been referenced as the fluorescence intensity of **4** at pH 7, and has been set to 1.

The fluorescence emission spectrum shown in **Figure 4.8** for neutral **171** (pH 14), has a residual fluorescence quantum yield of Φ = 0.046, similar to that of **146** and **170**.

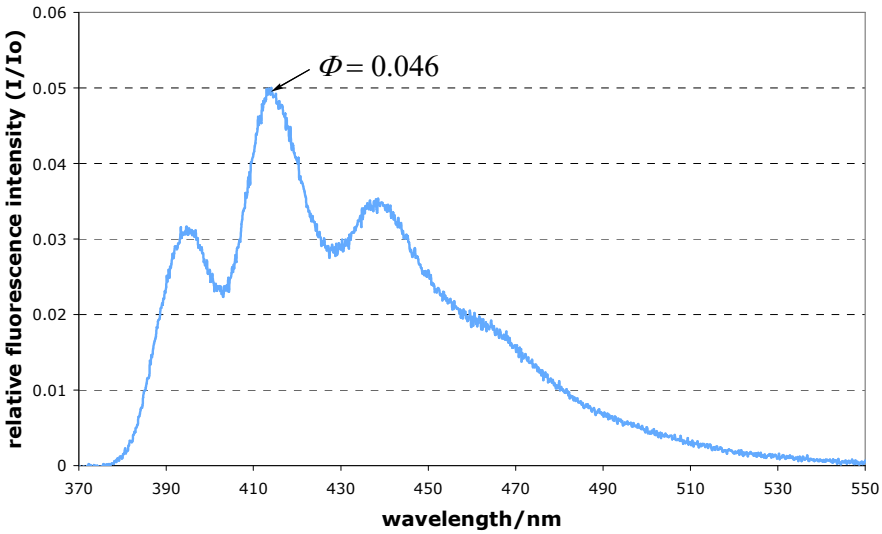

Figure 4.8. The fluorescence emission spectrum of **171** [1 x 10^{-6} mol dm^{-3}] at pH 14 in 20% aqueous 1,4-dioxane (I = 0.1 mol dm^{-3}, NEt_4ClO_4) at 298 K when excited at 350 nm. I_o has been referenced as the fluorescence intensity of **4** at pH 7, and has been set to 1.

As expected acidification of **171** produced an enhancement of the fluorescence as shown in **Figure 4.9**. Strongly acidic conditions (pH < 2) still causes a decrease of fluorescence, though only half what was seen for **146**. Interestingly,

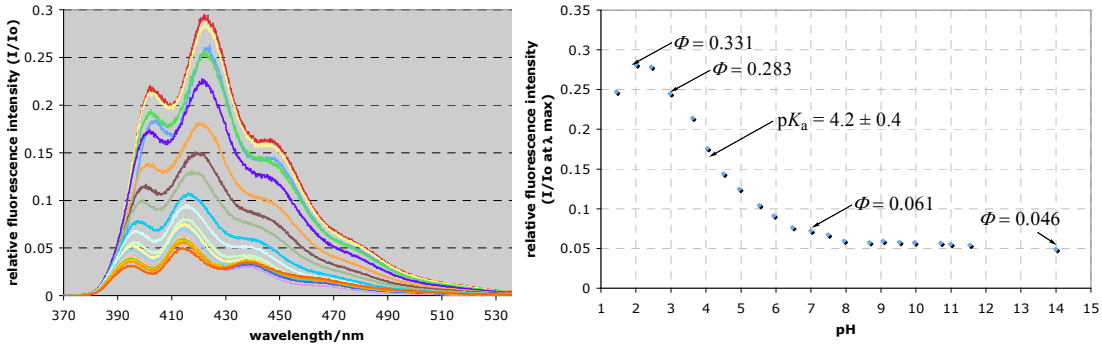

(a) **(b)**

Figure 4.9. **(a)** The fluorescence emission spectra during the titration of protonated **171** [1 x 10^{-6} mol dm^{-3}] with NEt_4OH in 20% aqueous 1,4-dioxane (I = 0.1 mol dm^{-3}, NEt_4ClO_4) at 298 K when excited at 350 nm. Emission maxima are at 403.2, 422.5 and 444.7 nm at pH 2 and at 394.5, 414.5 and 438.2 nm at pH 10. Maximum fluorescence emission intensity decreases from pH 2.0 (red curve) to pH 14.0 (orange curve); **(b)** Fluorescence intensity at λ_{max} plotted against pH, values derived from **Figure 4.9(a)**. I_o has been referenced as the fluorescence intensity of **4** at pH 7, and has been set to 1.

the plot of fluorescence emission intensity at λ_{max} versus pH shown in **Figure 4.9(b)**, whilst having the same sigmoidal shape as seen for **146** and **170**, is suggestive of a pK_a value of 4.2 ± 0.4 relating the strongly fluorescent and weakly fluorescent species. This can be explained by noting that the anthrylamine group in **146** and **170** is secondary, whereas in **171** it is tertiary and generally speaking tertiary amines are less basic than secondary amines.[261] It is not entirely clear why the pK_a difference is as large as it is, however, it is probably due, at least in part, to the inductive effect of the oxygen atom two carbon atoms away.[261] It must also be kept in mind that these values are not being recorded in water where both the behaviour of the glass electrode and the absolute values of pK_as are both better understood.

The fluorescence emission spectrum shown in **Figure 4.10** for **172** (pH =14), showed a quantum yield (Φ = 0.028) that was considerably lower than for **146**, **170** or **171**, but similar to that of **131** (Φ = 0.028), with the residual fluorescence only a 40% that of **146**.

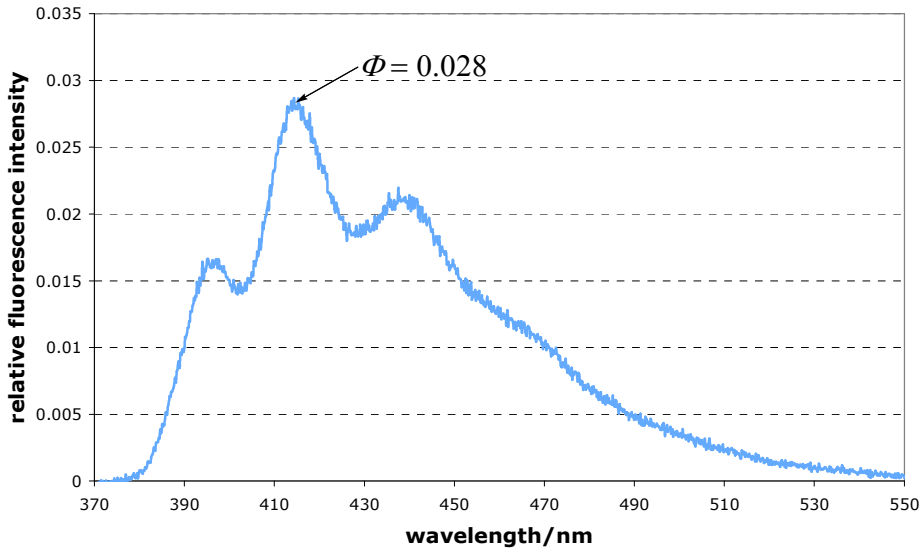

Figure 4.10. The fluorescence emission spectrum for **172** [1 x 10^{-6} mol dm^{-3}] at pH = 14 in 20% aqueous 1,4-dioxane (I = 0.1 mol dm^{-3}, NEt_4ClO_4) at 298 K when excited at 350 nm. I_o has been referenced as the fluorescence intensity of **4** at pH 7, and has been set to 1.

As expected acidification of **172** produced an enhancement of the fluorescence as shown in **Figure 4.11**. No decrease in fluorescence was observed in strongly acidic conditions. As with **171**, the plot of fluorescence emission intensity at λ_{max} versus pH shown in **Figure 4.11(b)** has the same sigmoidal shape and a pK_a value of 4.0 ± 0.2 relating the strongly and weakly fluorescent species, which is consistent with that of **171**.

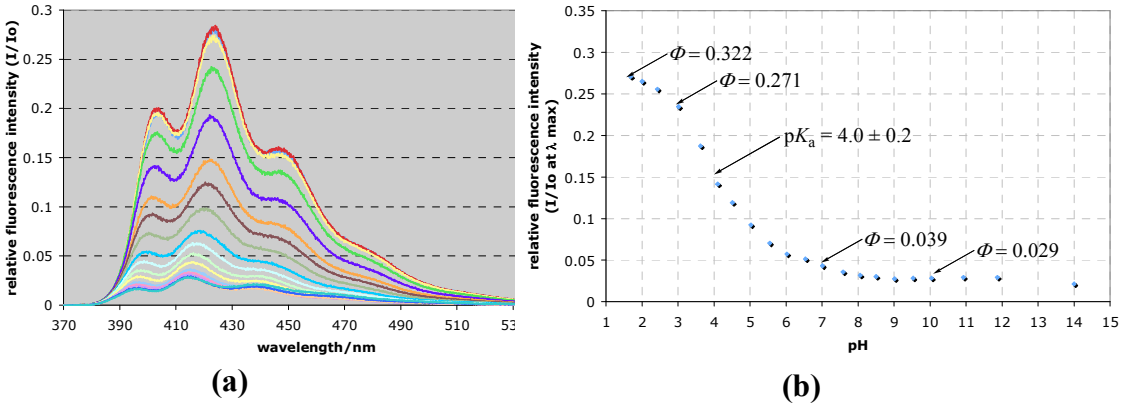

Figure 4.11. **(a)** The fluorescence emission spectra for the titration of the protonated **172** [1 x 10^{-6} mol dm^{-3}] against NEt_4OH in 20% aqueous 1,4-dioxane (I = 0.1 mol dm^{-3}, NEt_4ClO_4) at 298 K when excited at 350 nm. Emission maxima are at 403.5, 424.5 and 447.4 nm at pH 2 and at 396.1, 414.4 and 439.5 nm at pH 10. Maximum fluorescence emission intensity decreases from pH 1.7 (red curve) to pH 14.0 (blue curve); **(b)** Fluorescence intensity of **172** at λ_{max} plotted against pH, values derived from **Figure 4.11(a)**. I_o has been referenced as the fluorescence intensity of **4** at pH 7, and has been set to 1.

The fluorescence emission spectrum shown in **Figure 4.12** for neutral **173** (pH =14), showed a residual fluorescence quantum yield of Φ = 0.014.

Acidification of **173** produced an enhancement of the fluorescence as shown in **Figure 4.13**. As with **172** strongly acidic conditions did not cause a decrease in fluorescence. The plot of fluorescence emission intensity at λ_{max} versus pH shown in **Figure 4.13(b)** has the same sigmoidal shape and gives a pK_a value of 4.3 ± 0.5 relating the strongly and weakly fluorescent species. This value is similar to that of both **171** and **172**.

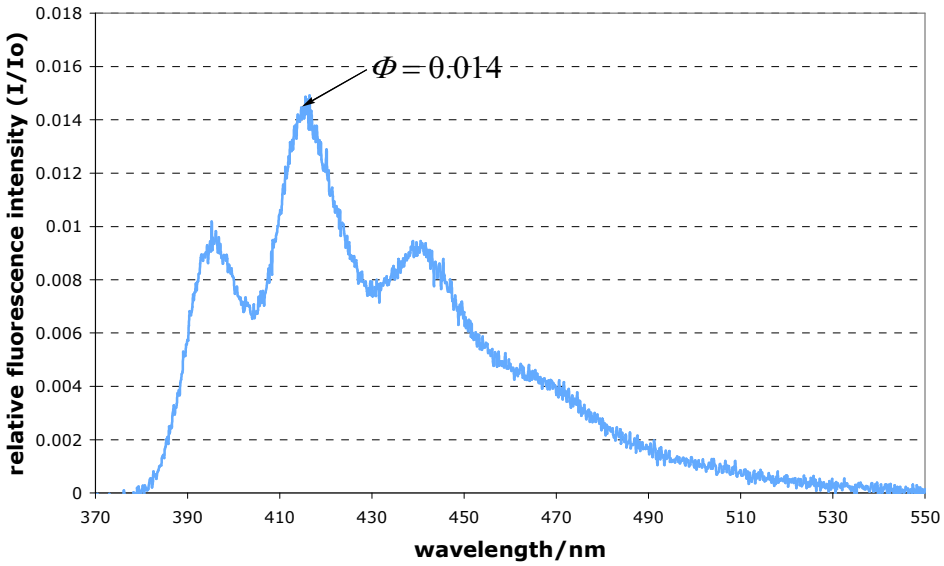

Figure 4.12. The fluorescence emission spectrum for **173** [1 x 10^{-6} mol dm^{-3}] at pH = 10 in 20% aqueous 1,4-dioxane (I = 0.1 mol dm^{-3}, NEt_4ClO_4) at 298 K when excited at 350 nm. I_o has been referenced as the fluorescence intensity of **4** at pH 7, and has been set to 1.

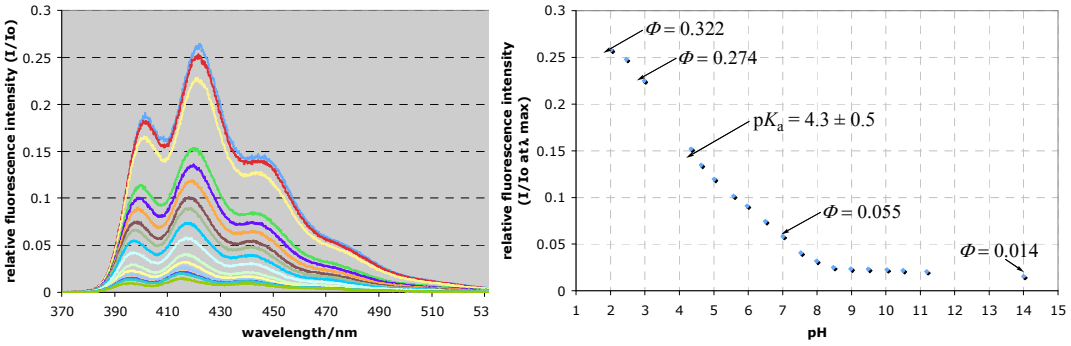

(a) **(b)**

Figure 4.13. **(a)** The fluorescence emission spectra during the titration of **173** [1 x 10^{-6} mol dm^{-3}] with NEt_4OH in 20% aqueous 1,4-dioxane (I = 0.1 mol dm^{-3}, NEt_4ClO_4) at 298 K when excited at 350 nm. Emission maxima are at 402.1, 422.8 and 445.3 nm at pH 2 and at 396.9, 417.0 and 442.9 nm at pH 10. Maximum fluorescence emission intensity decreases from pH 2.0 (blue curve) to pH 14.0 (green curve); **(b)** Fluorescence intensity of **173** at λ_{max} plotted against pH, values derived from **Figure 4.13(a)**. I_o has been referenced as the fluorescence intensity of **4** at pH 7, and has been set to 1.

The investigation of the effects of pH upon the ligands (**146**, **170-173**) revealed that protonation has a significant effect on the fluorescence spectra of the ligands, allowing these ligands to act as pH sensors within the region ± *ca* 2 pH units of the pH corresponding to the pK_a value. To avoid unwanted pH induced changes in both the absorption and fluorescence spectra, all subsequent examinations of

photospectroscopic properties of these ligands, and their derived complexes, were conducted in buffered solutions.

Table 4.1 tabulates the observed pK_a values for the protonated anthrylamine alongside the residual fluorescence at pH 14, where the ligands are likely to be in the fully deprotonated condition, although it is difficult to be certain of this in the non-aqueous conditions employed here. If these ligands were not fully deprotonated at the highest pH, the variation in residual fluorescence may be derived only from the differences in the degree or site of protonation of the ligands.

Table 4.1 The residual fluorescence quantum yields at pH 14 and apparent pK_a values for ligands **146**, **170-173** in 20% aqueous 1,4-dioxane, (I = 0.1 mol dm^{-3}, NEt_4ClO_4) at 298 K.

Ligand	pK_a	Quantum Yield (Φ), (pH 14) (residual fluorescence)
146	8.4 ± 0.4	0.069
170	8.0 ± 0.3	0.047
171	4.2 ± 0.4	0.046
172	4.0 ± 0.2	0.028
173	4.3 ± 0.5	0.014

It is seen that as the basicity of the anthrylamine drops (lower pK_a) the residual fluorescence drops, indicating that PeT quenching is becoming more efficient. This is somewhat surprising since reduced basicity implies reduced nitrogen lone pair availability, which in turn suggests that the residual fluorescence should be higher for the ligands of low basicity. However it may be explained in the following way: The Brønsted basicity of an amine, or in other words its ability to take on a proton is what is determined when a pH titration is used to evaluate the pK_a. On changing from a secondary amine to a tertiary amine the pK_a of an amine is generally seen to fall, as is the case here, due to increased steric crowding reducing the accessibility of the lone pair to the incoming proton. This is despite the fact that the extra alkyl or aryl group added as the tertiary amine forms ought to increase the

electron density at the nitrogen (these groups being electron releasing) making the amine more basic, although the electron donation to the tertiary amine is reduced by the effect of the oxygen atom just two carbon atoms away.

The fact that PeT quenching is becoming more efficient even though the pK_a is falling is suggestive of the fact that the steadily increasing electron donation as one moves from H (**146**), to 2-hydroxy-3-phenoxypropyl (**171**), to 2-hydroxy-3-[4'-(methyl)phenoxy]propyl (**172**), to 2-hydroxy-3-[4'-(*tert*-butyl)phenoxy]propyl (**173**) is indeed rendering the nitrogen atom more basic, but in the Lewis sense, only, and not in the Brønsted sense. Why **171** shows no decrease of residual quantum yield, compared to **170**, is not clear.

Figure 4.14 shows the fluorescence intensities at three different pH values for all the ligands under investigation. At the pK_a value, 50% of the ligand in solution is protonated at the anthrylamine, resulting in a half-way revival of fluorescence. It can be seen that even though the residual fluorescence emission intensities of the individual ligands vary widely depending on the electron density of the amine, the fluorescence emission intensities of the solutions with a pH corresponding to the pK_a value, appear to be grouped together in the two different groups. The ligands with a secondary anthrylamine, **146** and **170**, have very similar fluorescence emission intensities at their 50% protonated states, which are close to that of **131**. Meanwhile the *N*-alkylated ligands, with the more electron rich tertiary anthrylamine, **171**-**173**, all have similar fluorescence emission intensities to each other that are *ca* half that of the ligands **146** and **170**. This can be ascribed to the hydrogen bonding of the OH group (two carbons away from the tertiary anthrylamine) to the excited anthracene.

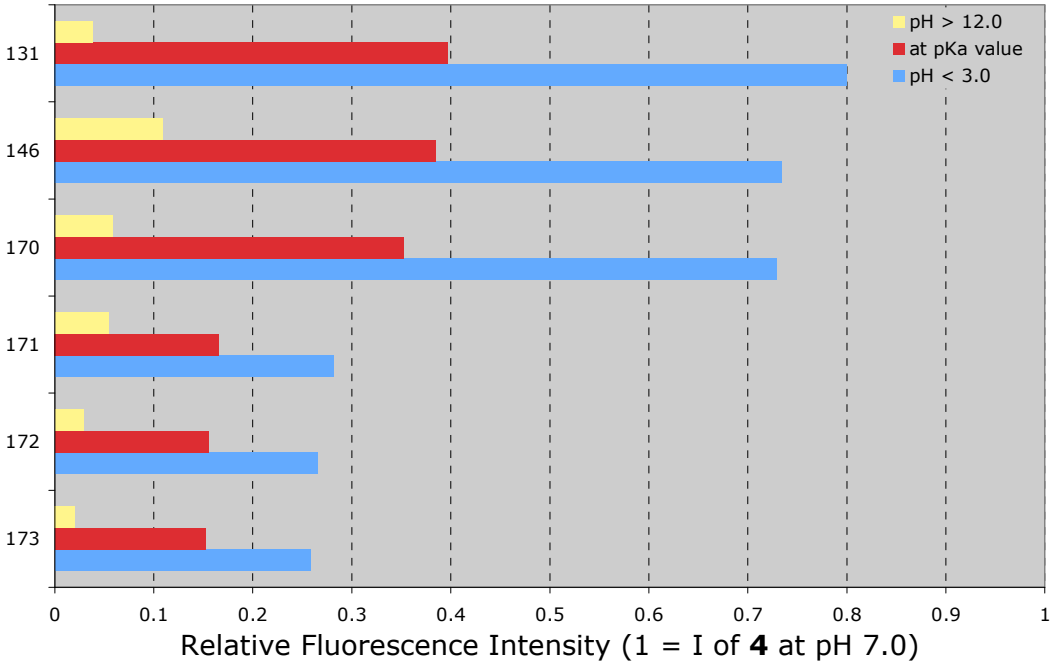

Figure 4.14. The fluorescence emission intensities of ligands **131**, **146**, and **170-173** at λ_{max}. At the pH values showing the lowest emission intensity (pH > 12, yellow bar), highest emission intensity (pH < 3, blue bar) and at the pH corresponding to the pK_a value for the ligand (red bar) for solutions of ligands [1 x 10^{-6} mol dm^{-3}] in 20% aqueous 1,4-dioxane (I = 0.1 mol dm^{-3}, NEt_4ClO_4) at 298 K when excited at 350 nm. The intensity values are given relative to the maximum fluorescence intensity of receptor **4**, the Cd(II)**146** complex, which has arbitrarily been set to 1.

4.3. Metal ion activated molecular sensors

Whilst ligands **146**, **170-173** can act as fluorescent pH sensors, the principal interest in these compounds lies in their basis as metal ion activated fluorescent molecular sensors, able to signal the inclusion of small guest molecules. Previous work,[114,115,122,125,242,262] as described in the introduction, has shown that metal complexation, leading to octa-coordination, causes the pendant arms to juxtapose to form a calixarene like cavity, capable of including small molecules. The ability of receptor complexes of this type to include various small molecules was described in **Chapter 3**, which detailed the use of NMR spectroscopy to monitor guest inclusion. Appropriate metal complexes of the ligands **146**, **170-173**, should be capable of

signalling guest inclusion through a change in the fluorescence, but to verify this it was first necessary to establish the fluorescence properties of the metal complexes that were to act as the host molecules.

4.3.1. The effect of metal complexation on fluorescence.

In this study the potentially eight-coordinating metal ions Cd(II), Hg(II) and Pb(II) were investigated for their influence on both the absorption and fluorescence properties of the ligands **146**, **170-173**. The potentially six-coordinating Zn(II) ion was also examined for comparative purposes. From previous work it is well known that when the metal ions under consideration bind to ligands of the type **146**, **170-173** they bind to all four nitrogen atoms in the cyclen residue and up to four of the four pendant donor atoms. In the event that the pendant anthrylamine does not coordinate to the metal atom it would be possible for it to exist in either the protonated or deprotonated form, depending upon the prevailing pH. In the previous section it has been shown that minor pH variations around the pK_a value of the pendant anthrylamine cause major shifts in the fluorescence emission intensity of the ligand. Thus it was important in investigating the fluorescence of metal complexes of **146**, **170-173** to buffer the solution at some arbitrarily chosen pH so as to avoid fluorescence changes arising from pH change (which may arise due to metal ion hydrolysis), which would mask the changes due to the metal ion complexation. For this purpose it was decided to buffer the solutions at pH 7.0 using HEPES (4-(2-hydroxyethyl)-1-piperazine-ethanesulfonic acid). HEPES was chosen as it is known to be resistant to metal ion complexation and would thus control the pH without interfering with the investigation.[53,151,263]

The interaction of ligands **146** and **170-173** (1 x 10^{-4} mol dm^{-3}) with Cd(II) (0-5 equiv) was examined by UV-visible absorption titrations at 25°C. The absorption of **146** showed only a slight increase in molar absorptivity upon addition of Cd(II), which plateaued at one equivalent of Cd(II), as shown in **Figure 4.15.**

The interaction of **146** (1 x 10^{-6} mol dm^{-3}) with Cd(II) (0-5 equiv) was also examined by fluorometric signalling at 25°C to see how the Cd(II) coordination would effect the PeT from the anthrylamine. As anticipated, the emission of **146** increased until one equivalent of Cd(II) had been added, and no further increase was observed at higher concentrations of Cd(II), as shown in **Figure 4.16.**

The fluorescence quantum yield of **146** at pH 7.0 increased by 45% with the addition of one equivalent of Cd(II) (Φ = 0.471 $\rightarrow$0.684), as shown in **Figure 4.16**.

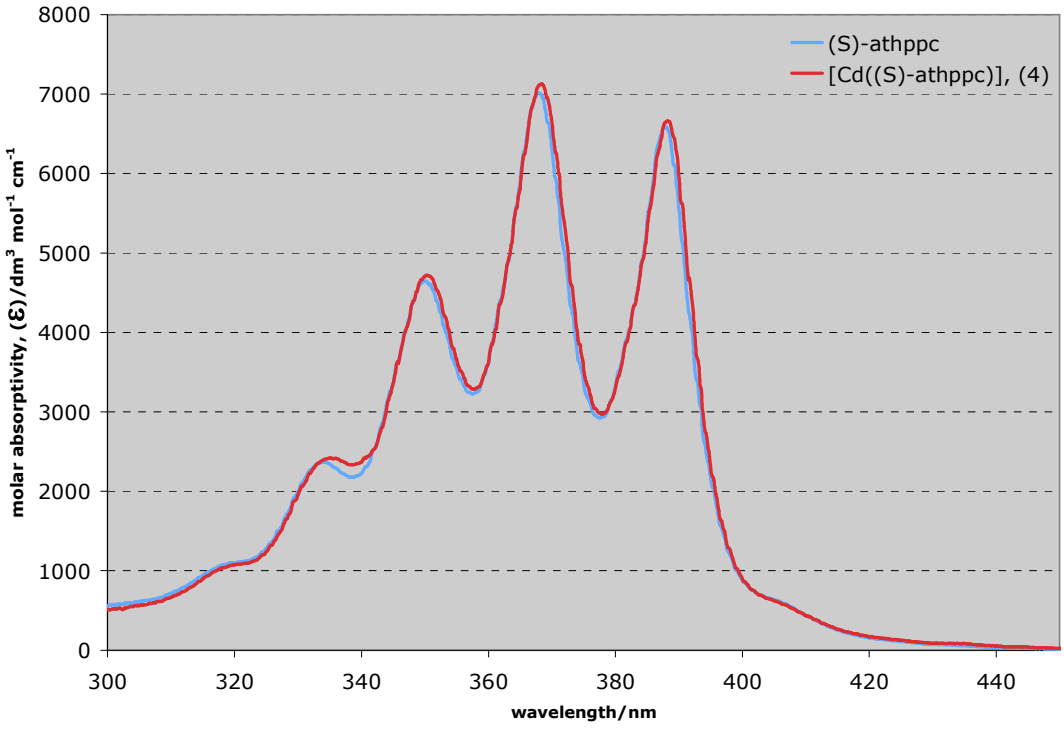

Figure 4.15. The absorption spectra of **146** (1 x 10^{-4} mol dm^{-3}) alone (blue trace) and with Cd(II) (1 x 10^{-4} mol dm^{-3}) (red trace) in 20% aqueous 1,4-dioxane, I = 0.1 mol dm^{-3} (NEt_4ClO_4), at pH 7.0 (0.01 mol dm^{-3} HEPES).

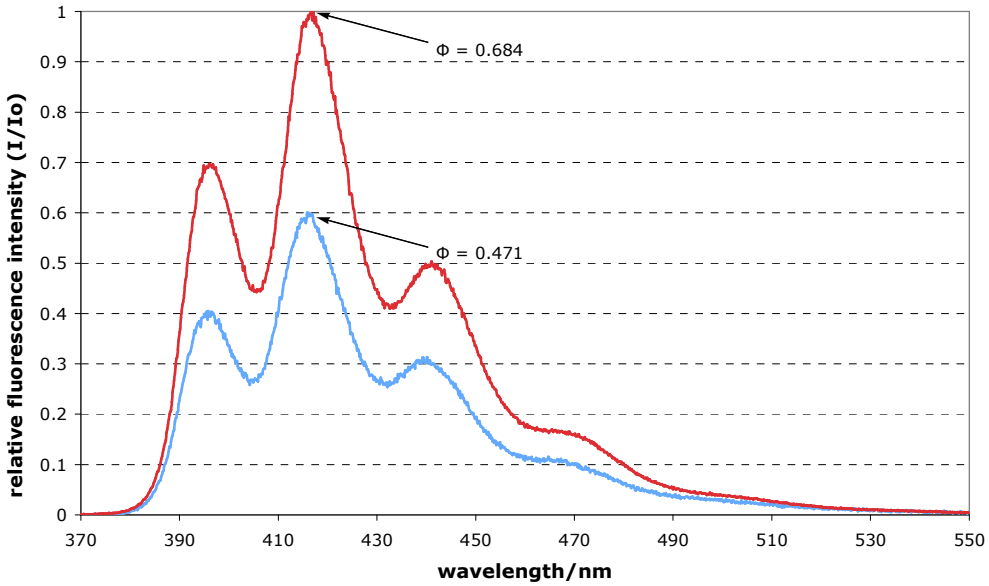

Figure 4.16. The fluorescence emission spectra and quantum yields (Φ) of a solution of **146** (1 x 10^{-6} mol dm^{-3}) alone (blue trace) and with Cd(II) (1 x 10^{-6} mol dm^{-3}) (red trace) in 20% aqueous 1,4-dioxane, I = 0.1 mol dm^{-3} (NEt_4ClO_4), at pH 7.0 (0.01 mol dm^{-3} HEPES). I_o has been referenced as the fluorescence intensity of **4** at pH 7, and has been set to 1.

Since the solution is buffered this must be due to metal coordination and not protonation. The fluorescence emission intensity increase is accounted for by the Cd(II) coordination of the anthrylamine, which restricts its PeT. The fluorescent response to Pb(II) and Zn(II) under the same conditions was smaller, with both resulting in a 10% increase in fluorescence quantum yield (Φ = 0.518), while the addition of Hg(II) caused a diminution of fluorescence emission intensity (Φ = 0.358) from that shown by the ligand itself at pH 7.0.

In the same way the interaction of **170** (1 x 10^{-6} mol dm^{-3}) with Cd(II) (0-5 equiv) was examined by fluorometric signalling at 25°C to see how the Cd(II) coordination would effect the PeT from the anthrylamine. As anticipated, the fluorescence emission intensity of **170** increased until one equivalent of Cd(II), and no further increase was observed at higher concentrations of Cd(II). The quantum yield of **170** at pH 7.0 increased by 34% with the addition of one equivalent of Cd(II) (Φ = 0.406 $\rightarrow$0.546), as shown in **Figure 4.17.**

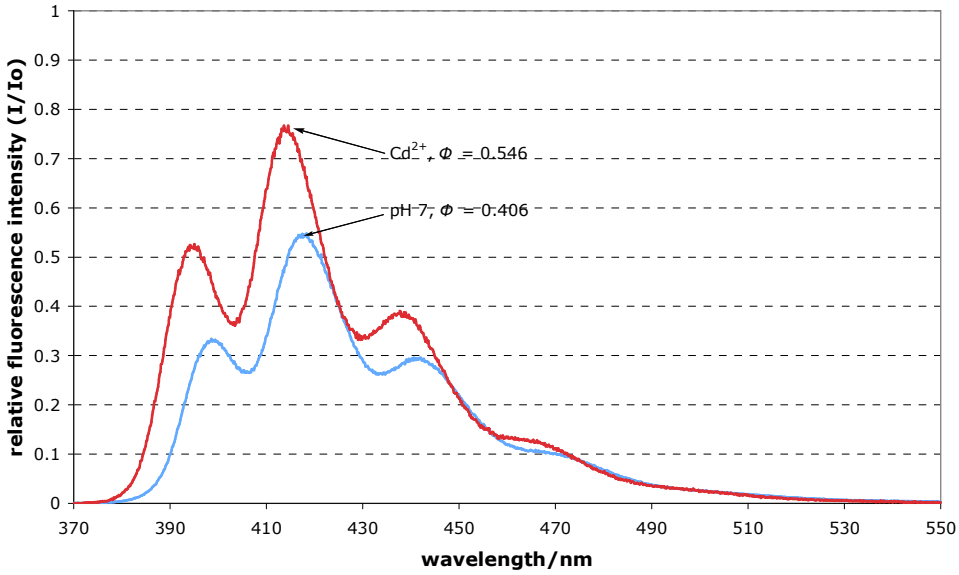

Figure 4.17. The fluorescence emission spectra and quantum yields (Φ) for a solution of **170** (1 x 10^{-6} mol dm^{-3}) alone (blue trace) and with Cd(II) (1 x 10^{-6} mol dm^{-3}) (red trace) in 20% aqueous 1,4-dioxane, I = 0.1 mol dm^{-3} (NEt_4ClO_4), at pH 7.0 (0.01 mol dm^{-3} HEPES). I_o has been referenced as the fluorescence intensity of **4** at pH 7, and has been set to 1.

The interaction of **171** (1 x 10^{-6} mol dm^{-3}) with Cd(II) (0-5 equiv) was examined by fluorometric signalling at 25°C to see how the Cd(II) coordination would effect the PeT from the anthrylamine. As anticipated, the fluorescence emission intensity of **171** increased until one equivalent of Cd(II) had been added, and no further increase was observed at higher concentrations of Cd(II). The quantum yield of **171** at pH 7.0 increased 311% with the addition of one equivalent of Cd(II) (Φ = 0.061 $\rightarrow$0.251), as shown in **Figure 4.18**. The fluorescent response to Pb(II) under the same conditions resulted in a 233% increase in fluorescence emission intensity (Φ = 0.203).

The interaction of **172** (1 x 10^{-6} mol dm^{-3}) with Cd(II) (0-5 equiv) was examined by fluorometric signalling at 25°C to see how the Cd(II) coordination would effect the PeT from the anthrylamine. As anticipated, the fluorescence emission intensity of **172** increased until one equivalent of Cd(II) had been added, and no further increase was observed at higher concentrations of Cd(II). The

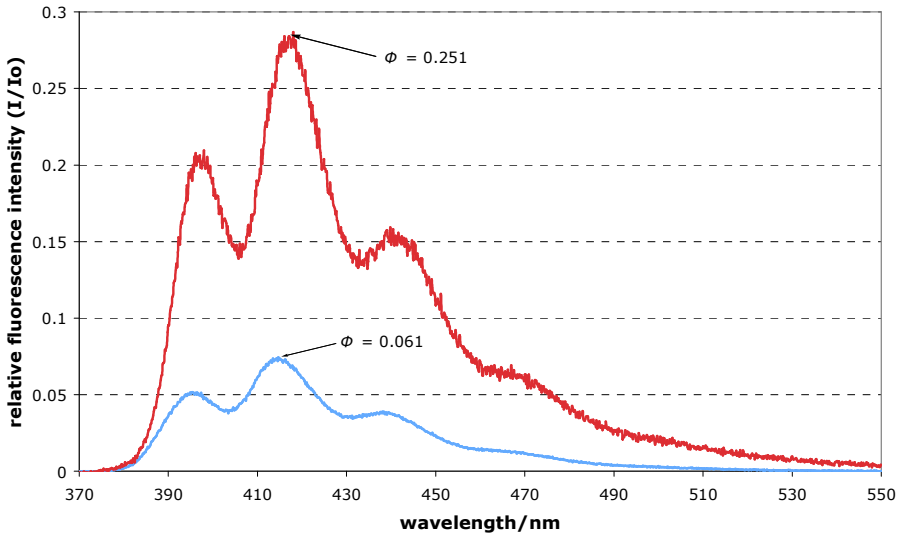

Figure 4.18. The fluorescence emission spectra and quantum yields (Φ) of a solution of **171** (1 x 10^{-6} mol dm^{-3}) alone (blue trace) and with Cd(II) (1 x 10^{-6} mol dm^{-3}) in 20 % aqueous 1,4-dioxane, I = 0.1 mol dm^{-3} (NEt_4ClO_4), at pH 7.0 (0.01 mol dm^{-3} HEPES). I_o has been referenced as the fluorescence intensity of **4** at pH 7, and has been set to 1.

quantum yield of **172** at pH 7.0 increased by 525% with the addition of one equivalent of Cd(II) (Φ = 0.039 →0.244), as shown in **Figure 4.19**. The fluorescent response to Pb(II) under the same conditions resulted in a 500% increase in fluorescence emission intensity (Φ = 0.230).

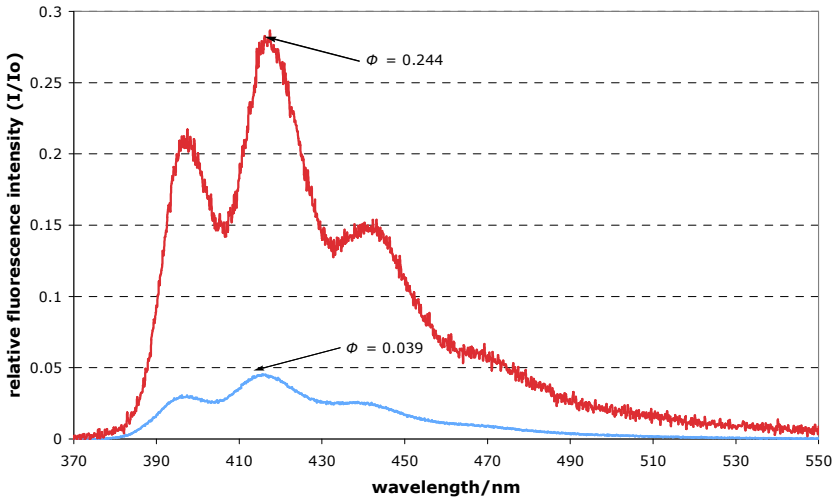

Figure 4.19. The fluorescence emission spectra and quantum yields (Φ) of a solution of **172** (1 x 10^{-6} mol dm^{-3}) alone (blue trace) and with Cd(II) (1 x 10^{-6} mol dm^{-3}) (red trace) in 20 % aqueous 1,4-dioxane, I = 0.1 mol dm^{-3} (NEt_4ClO_4), at pH 7.0 (0.01 mol dm^{-3} HEPES). I_o has been referenced as the fluorescence intensity of **4** at pH 7, and has been set to 1.

The interaction of **173** (1 x 10^{-6} mol dm^{-3}) with Cd(II) (0-5 equiv) was examined by fluorometric signalling at 25°C to see how the Cd(II) coordination would effect the PeT from the anthrylamine. As anticipated, the fluorescence emission intensity of **173** increased until one equivalent of Cd(II) had been added, and no further increase was observed at higher concentrations of Cd(II). The quantum yield of **173** at pH 7.0 increased by 338% with the addition of one equivalent of Cd(II) (Φ = 0.055 →0.241), as shown in **Figure 4.20**.

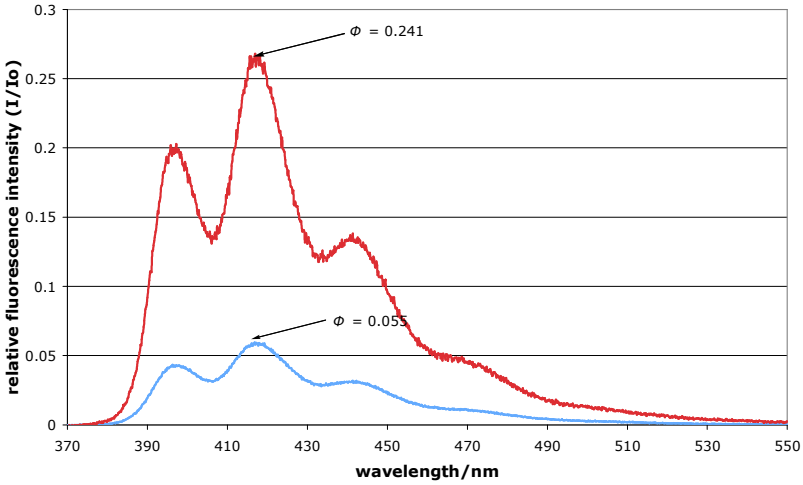

Figure 4.20. The fluorescence spectra and quantum yields (Φ) of the titration of a solution of **173** (1 x 10^{-6} mol dm^{-3}) alone (blue trace) and with Cd(II) (1 x 10^{-6} mol dm^{-3}) (red trace) in 20 % aqueous 1,4-dioxane, I = 0.1 mol dm^{-3} (NEt_4ClO_4), at pH 7.0 (0.01 $moldm^{-3}$ HEPES). I_o has been referenced as the fluorescence intensity of **4** at pH 7, and has been set to 1.

A comparison of the relative fluorescence intensities for all the ligands with a variety of metal(II) ions is given in **Figure 4.21.** It shows that Cd(II) generally invokes the largest increase in intensity. In all cases the fluorescence emission intensity of the Cd(II) complexes is greater than the maximum fluorescence intensity of the ligand shown at low pH (pH 2-3). The fluorescence emission intensities can also be compared to those of **131**, which behave differently. In water at pH 7.4, **131**[151] showed a 40% increase in fluorescence emission intensity for the complexation of Cd(II), the complexation of Pb(II) caused a 25% diminution of the fluorescence emission intensity, the complexation of Hg(II) caused *ca* 90%

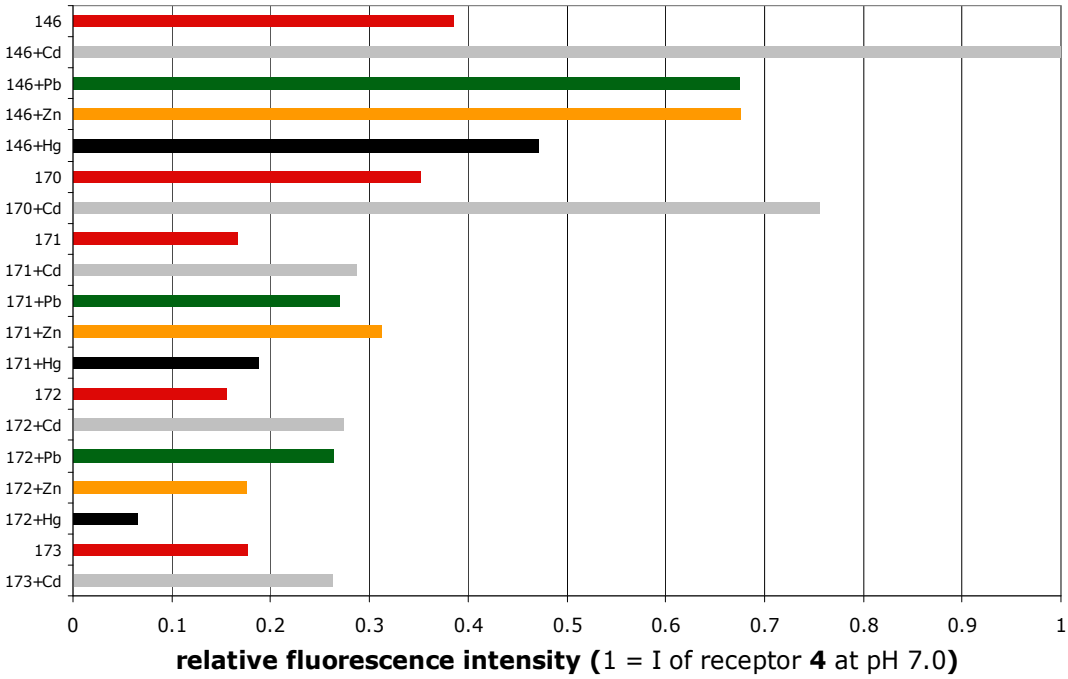

Figure 4.21. Relative fluorescence intensity at 416 nm of **146**, **170-173** responding to 1 equiv of metal ions at 25°C in 20% aqueous dioxane, I = 0.1 mol dm^{-3} (NEt_4ClO_4), at pH 7.0 (0.01 mol dm^{-3} HEPES). The red bars depict the fluorescence emission intensity of the free ligands at the pH that corresponds to their observed pK_a values. The fluorescence emission intensity values are given relative to the maximum fluorescence intensity of the Cd(II) complex of **146**, which has arbitrarily been set as 1.

diminution of fluorescence emission intensity. Complexation of Zn(II) resulted in the greatest fluorescence emission intensity increase of 220%.

This trend in fluorescence increase of Zn(II) > Cd(II) > Pb(II) > Hg(II) is not continued for the ligands containing four pendant arms, **146**, **170-173**. For example, when using the fluorescence of **146** at its pK_a value (8.4), as the reference, the fluorescence emission intensity for Cd(II) complexation showed a 160% increase, 76% for Zn(II), 75% for Pb(II), and 22% for Hg(II). This may be attributed to the fact that whilst Cd(II), Pb(II) and Hg(II) are all potentially eight-coordinate, and are able to bind with the four nitrogens of the cyclen residue and all four pendant arms, Zn(II) cannot. There is a high probability that a significant amount of the anthrylamine will not be complexed, resulting in a lower fluorescence.

With the fluorescence properties of the receptor ligands and receptor complexes examined, the study of the fluorescence perturbation induced in the receptor complex by the inclusion of guest anions could now be undertaken.